HHS Public Access

Author manuscript

Nat Struct Mol Biol. Author manuscript; available in PMC 2012 October 01.

Published in final edited form as:

Nat Struct Mol Biol. ; 19(4): 387–394. doi:10.1038/nsmb.2245.

A Telomere Dependent DNA Damage Checkpoint Induced by Prolonged Mitotic Arrest

Makoto T. Hayashi[1], **Anthony J. Cesare**[1], **James A. J. Fitzpatrick**[2], **Eros Lazzerini-Denchi**[3], and **Jan Karlseder**[1]

[1]The Salk Institute for Biological Studies, Molecular and Cellular Biology Department, 10010 North Torrey Pines Rd., La Jolla, CA92037,USA

[2]The Salk Institute for Biological Studies, Waitt Advanced Biophotonics Center, 10010 North Torrey Pines Rd., La Jolla, CA92037, USA

[3]The Scripps Research Institute, Department of Genetics, 10550 North Torrey Pines Road, La Jolla, CA92037, USA

Summary

Telomere shortening and disruption of telomeric components are pathways that induce telomere deprotection. Here we describe another pathway, where prolonged mitotic arrest induces damage signals at telomeres in human cells. Exposure to microtubule drugs, kinesin inhibitors, proteasome inhibitors or the disruption of proper chromosome cohesion resulted in the formation of damage-foci at telomeres. Induction of mitotic telomere deprotection coincided with dissociation of TRF2 (Telomere Repeat binding Factor 2) from telomeres, telomeric 3'-overhang degradation and ATM (Ataxia Telangiectasia Mutated) activation, and could be suppressed by TRF2 overexpression or inhibition of Aurora B kinase. Normal cells that escape from prolonged mitotic arrest halted in the following G1 phase, whereas cells lacking p53 continued to cycle and became aneuploid. We propose a telomere dependent mitotic duration monitoring system that reacts to improper progression through mitosis.

Introduction

To avoid unwanted checkpoint activation by natural chromosome ends, cells have evolved telomeres. Human telomeres are composed of double stranded TTAGGG repeats and a single stranded G rich 3' overhang, which are covered and protected by shelterin [1]. Among the six shelterin components TRF2 and POT1 (Protection Of Telomeres 1) have predominantly been implicated in chromosome end protection by preventing ATM- and

Correspondence should be addressed to J.K. (Karlseder@salk.edu).

Author Contributions

MTH designed and carried out experiments and wrote the manuscript, AJC designed and carried out experiments and wrote the manuscript, JAJF provided imaging expertise, ELD designed and carried out experiments, JK designed experiments and wrote the manuscript.

Competing financial interests

The authors declare no competing financial interests.

ATR (Ttaxia Telangiectasia and Rad3 related)-dependent checkpoint activation [2–5]. Upon disruption of TRF2 or POT1 telomeres are recognized as sites of DNA damage, resulting in phosphorylation of histone H2AX (γ-H2AX) within the telomeric and sub-telomeric chromatin and association of 53BP1 (p53 Binding Protein) with the chromosome ends. The co-localization of DNA-damage response factors and chromosome ends can be visualized as telomere dysfunction-induced foci (TIF) [6]. TIF have also been intimately linked to replicative senescence [7] and shown to occur spontaneously in cancer cell lines [8].

Cells arrested in mitosis are known to either die during mitotic arrest, or skip cytokinesis and "slip" into the subsequent G1 phase of the cell cycle [9]. Mitotic slippage occurs through the degradation of Cyclin B1 in the presence of the active spindle assembly checkpoint (SAC) [10]. Cells that exit from prolonged mitotic arrest or progress through mitotic slippage exhibit various fates, including apoptosis or p53-dependent cell cycle arrest [9,11]. In both normal and cancer cells, cell death during mitotic arrest, or apoptosis or senescence after escape from prolonged mitotic arrest are crucial for preventing chromosome instability. A failure to remove cells from the cycling population following prolonged mitotic arrest may allow cells to continue propagating with an abnormal number of chromosomes [12–14]. However, despite intense research, the molecular mechanisms that trigger growth arrest or death in mitotically arrested cultures have not yet been identified.

We set out to explore putative telomeric functions for cohesin and found that mitotic arrest per se induces telomere deprotection in primary and transformed human cells. Telomere deprotection during mitotic arrest associated with loss of the telomeric 3'-overhangs, led to ATM activation and was ATM dependent. TRF2 was dissociated from telomeres during prolonged mitotic arrest, providing the molecular basis for overhang loss and ATM activation, which was emphasized by the finding that TRF2 overexpression protected telomeres from the damage machinery during mitotic arrest.

Inhibition of Aurora B kinase suppressed the telomere deprotection phenotype, but independent of the involvment of the SAC. Cells suffering from mitotic telomere deprotection underwent p53 dependent cell cycle arrest in the following G1 phase after mitotic release, while cells lacking p53 function continued to cycle and became aneuploid. Our findings provide a molecular mechanism explaining the induction of DNA damage signaling, cell cycle arrest or apoptosis following prolonged mitotic arrest, and explain the mechanism of action of therapeutic drugs, such as Taxol, Vinblastine and Velcade, which all inhibit mitotic progression. We propose that telomeric destabilization during mitotic arrest induces DNA damage signaling and potentially serves as a mitotic duration checkpoint, responsible for eliminating cells that fail to progress through mitosis properly.

Results

Prolonged mitotic arrest induces telomeric DNA damage foci

Cohesin, composed of the core subunits SMC1 (Structural Maintenance of Chromosomes 1), SMC3, RAD21-SCC1 (Sister Chromatid Cohesion 1) and SCC3, was originally found to prevent premature sister chromosome separation during mitosis [15,16] and has also been shown to be involved in checkpoint activation, damage repair and recombination [17–20].

Thus, we asked whether cohesin functions were involved in telomeric protection. HeLa1.2.11 cells were subjected to knockdown of RAD21 (Fig. 1a, upper panel), resulting in premature sister chromatid separation and a mitotic arrest phenotype [21]. Mitotic cells were spread by cytocentrifugation and stained for γ-H2AX immuno-fluorescence (IF) and telomere fluorescent in situ hybridization (FISH) to visualize potential TIF on prometaphase-like nuclei (meta-TIF) [8]. Multiple TIF were observed when RAD21 was suppressed (Fig. 1b, upper right panels) in contrast to mock- and a non-silencing siRNA treated cells (Fig. 1b, upper left panels). Quantitation of the TIF revealed a four-fold increase in damage signals on all chromosome ends, and a nine-fold increase at the telomeres of mitotic nuclei with prematurelly separated sister chromatids, which are about 40% of the population and indicative of efficient cohesin knockdown (Fig. 1c, left panel). To distinguish, which function of cohesin is involved in this phenotype, we focused on sororin and shugoshin. Sororin is required for sister chromatid cohesion and for DSB (double stranded break) repair, but unlike cohesin, sororin is dispensable for checkpoint activation [20,22]. Shugoshin is required for maintenance of cohesin at centromeres in mitosis, but is dispensable for checkpoint and repair functions [22]. Sororin and shugoshin were both efficiently suppressed by siRNA targeting (Fig. 1a, lower panel). Both knockdowns induced premature sister chromatid separation and a ten fold increase in meta-TIF (Fig. 1b, lower panels and Fig.1c, middle panel).

This suggested that either cohesin, sororin and shugoshin are directly involved in telomere protection, or that mitotic arrest induced by the knockdowns indirectly caused telomere deprotection. We therefore treated HeLa1.2.11 cells with the microtubule destabilizing drug colcemid, which also arrests cells in mitosis. This treatment led to a similar increase in meta-TIF formation as observed upon the suppression of cohesin, sororin and shugoshin (Fig. 1c, right panel and Supplementary Fig. 1a), suggesting that it was the prolonged mitotic arrest that was the major cause of the meta-TIF phenotype.

Primary cells also exibit telomere deprotection following prolonged arrest in M phase. Colcemid addition to primary human diploid lung fibrobrast (IMR90) led to the formation of multiple TIF (Fig. 1d) in a time dependent manner (Fig. 1e and Supplementary Fig. 2a), in extreme cases leading to the deprotection of almost all telomeres (Supplementary Fig. 1b). γ-H2AX did not accumulate at non telomeric sites (Fig. 1e and Supplementary Fig. 2a). Human mammary epithelial cells (HMEC) displayed the same telomere deprotection phenotype (Supplementary Fig. 2b).

To examine meta-TIF formation dynamics IMR90 cells were synchronized at the G1-S boundary and cell cycle progression and mitosis entry was determined by histone H3 serine10 phosphorylation (H3-Ser10P) and DNA content (Supplementary Fig. 2c). Cells entered mitotis 8–12 h post release and re-entered G1 by 14 hrs. Colcemid was added at the 6 h time point, and meta-TIF formation in mitotic nuclei was determined at 10, 16 and 30 h (Fig. 2a). At 10 h post relase only background levels of telomeric and non-telomeric γ-H2AX foci were observed, suggesting that perturbation of microtubules during G2 has no effect on telomeres (Fig. 2b, no drug and colcemid panels and Supplementary Fig. 3). Cells started suffering an average of 12 and 23 meta-TIF at the 16 h and 30 h time points post release, respectively (Fig. 2b, colcemid panel and Supplementary Fig. 3). This again

indicates that deprotected telomeres accumulate during mitotic arrest but not in G2. Irradiation of mitotic cells at 10 h post release induced non-telomeric γ-H2AX foci, excluding the possibility that only the telomeric region is competent for γ-H2AX foci formation during mitosis (Fig. 2b, 1Gy IR panel and Supplementary Fig. 3).

Mitotic inhibitors such as vinblastine, taxol and velcade are frequently used as cancer therapy. Vinblastine depolymerizes microtubules, while taxol stabilizes them [23] and the proteasome inhibitor velcade blocks proteolysis of anaphase promoting complex (APC) substrates, leading to arrest at the metaphase-anaphase transition [24]. Dimethylenastron is a kinesin Eg5 inhibitor, which blocks centrosome segregation and causes monopolor kinetochore formation [25]. Since velcade appears to affect G2 progression as well, we added velcade at the 8 h time point when cells have started entering M phase (Fig. 2a). All drugs caused meta-TIF formation at 16 and 30 h, except for velcade, which led to a poor mitotic index 30 h post release, likely due to side effects of proteasome inhibition (Fig. 2b and Supplementary Fig. 3).

We suggest that the induction of the meta-TIF phenotype is independent of the pathways that lead to mitotic arrest, and that it is the length of time spent in mitosis that causes telomere deprotection.

Mitotic arrest causes 3'-overhang loss and ATM activation

To study whether the 3’-overhang was affected during prolonged mitosis, we colcemid-treated synchronized IMR90 cells and IMR90 cells expressing papilloma virus serotype 16 (HPV16) E6 and E7 proteins (IMR90 E6E7). Cells were harvested 0, 10 and 24 h post release, either by collection of the total sample or via mitotic shake-off (Fig. 3a) and the overhang status was analyzed [26]. We observed an approximate 50% reduction of overhang signal at the 24 h time point (Fig. 3b), likely in the mitotic fraction of cells, since the samples collected by mitotic shake-off exhibited an even more extensive loss of the 3’-overhang signal (Fig. 3b). Exonuclease I treatment confirmed that the telomeric signal from native hybridization stemmed from the 3’-overhangs and no detectable change in double stranded telomeric length was observed (Supplementary Fig. 4).

To demonstrate that telomeric ends, but not internal telomeric sequences, are required for the mitotic TIF phenotype, we suppressed TRF2 in IMR90 E6E7 cells (Fig. 3c). Meta-TIF analysis following colcemid exposure demonstrated that the internal telomeric sequences caused by TRF2 knockdown-induced telomere fusions do not induce a DNA damage signal (Fig. 3d, e). This supports the hypothesis that telomeric ends, but not internal telomeric sequences or subtelomeric regions, are involved in the meta-TIF phenotype.

To study the checkpoint response during mitotic arrest, synchronized IMR90 cells with or without colcemid exposure were analyzed by western blotting. In the presence of colcemid, H3-Ser10P accumulated gradually at the 8, 12, 16 and 30 h time points (Fig. 3f), indicating an accumulation of cells in mitosis. Elevation of γ-H2AX expression was observed after 16 and 30 h, similar to ATM autophosphorylation (ATM-Ser1981P) (Fig. 3f). Exposure of unsynchronized IMR90 cells to colcemid confirmed that ATM activation was concomitant

with the induction of telomere deprotection and not simply a side-effect of synchronization (data not shown).

Meta-TIF analysis of SV40-immortalized ATM-deficient fibroblasts (A-T SV40) suggested that ATM is required for telomeric γ-H2AX focus formation during mitotic arrest (Fig. 4a; upper panels). Quantification of γ-H2AX foci indicated that the A-T SV40 cells suffered from a greater number of non-telomeric γ-H2AX foci compared to IMR90 cells (Fig. 4b; non-TEL panels), but no increase in TIF formation was observed after 24 h of colcemid exposure (Fig. 4b; TEL panels), despite equal efficiency of the mitotic arrest (Supplementary Fig. 5a). Moreover, an immortalized A-T fibroblast cell line expressing HPV 16 E6 and E7 (A-T E6E7) failed to increase telomeric γ-H2AX foci after 24 h of colcemid treatment (Fig. 4b) and shRNA-mediated suppression of ATM in HeLa1.2.11 cells reduced the number of telomeric γ-H2AX foci after 24 h of colcemid exposure (Fig. 4c, d).

An immortalized HPV16 E6 and E7 expressing Seckel syndrome fibroblast cell line with a hypomorphic mutation in the ATR pathway (Seckel E6E7) showed an acute increase of telomeric γ-H2AX foci after prolonged mitotic arrest (Fig. 4a, lower panels), comparable to IMR90 cells (Fig. 4b). We therefore concluded that ATM, but not ATR, activation during mitotic arrest is upstream of H2AX phosphorylation at telomeric ends. However, due to the hypomorphic nature of the mutation in the Seckel cells we cannot completely exclude a partial contribution by the ATR pathway.

Prolonged mitotic arrest dissociates TRF2 from telomeres

Overhang loss and ATM activation are reminiscent of cells expressing a dominant negative allele of TRF2 (refs. 2, 3). We therefore asked whether TRF2 was still localized to telomeres after prolonged mitotic arrest. Synchronized IMR90 cells were subjected to chromatin immunoprecipitation (ChIP) analysis with antibodies against TRF1, TRF2 and histone H3. Histone H3 was detected at the telomeric and ALU repeats in all conditions tested, excluding the possibility that colcemid treatment changes the accessiblity of chromatin to antibodies (Fig. 5a, b). TRF2 binding to telomeric repeats was reduced by approximately 50% at the 30 hour time point, (Fig. 5a, b, TTAGGG panel). Conversely, forced retroviral expression of TRF2 (Fig. 5c) led to a reduction of meta-TIF to almost background levels in asynchronous and synchronized cells (Fig. 5d), while leaving the efficiency of mitotic arrest unchanged (not shown), emphasizing the central role that TRF2 plays in suppressing meta-TIF formation.

TRF1 levels at telomeric repeats were also slightly reduced during mitotic arrest (Fig. 5b). However, we do not suspect a role for TRF1 in this phenotype, since TRF1 overexpression did not substantially rescue the TIF phenotype (not shown), which is in accordance with the lack of a major role for TRF1 in telomere protection [27]. We also examined whole cell extracts of IMR90 cells exposed to colcemid up to 36 h and found no evidence for downregulation of shelterin components at the protein level (Supplementary Fig. 6a). We suggest that TRF2 is partially removed from telomeres during prolonged mitotic arrest, probably due to posttransrational regulation and not simply by protein degradation.

p53-dependent G1 arrest of cells with meta-TIF

Cells suffering from IR (Ionizing Radiation)-induced DNA damage in mitosis activate the checkpoint response in the following G1 phase [28]. To examine whether meta-TIF induced by mitotic arrest persist into G1 after release, mitotic IMR-90 cells were collected by shake off, re-plated and cultured. TIF were evident in arrested mitotic cells and the rounded cells and recently divided cells two to six hours after shake off. TIF became less evident eight hours post-shake off and were almost gone by ten hours (Fig. 6a). This suggests that TIF persist into early G1-phase before eventual repair. As a control, mitotic cells fixed 10 h after release from the double-thymidine bock without colcemid treatment exhibit no meta-TIF phenotype.

To address checkpoint activation in the following cell cycle we monitored p53 and p21 in IMR90 cells at the 24 and 48 h time points post release from a prolonged mitotic arrest (Fig. 6b). Cells shaken-off at the 10 h time point showed a slight increase in p53 and p21 levels after a 24 h recovery period, which diminished after 48 h (Fig. 6c). In contrast, when mitotic cells were collected at the 16 h time point, activation of p53 (p53-Ser15P) and a strong p53 and p21 accumulation could be detected up to 48 h (Fig. 6c). This suggests that prolonged mitotic arrest caused a p53-dependent cell cycle arrest in the following G1 phase.

To examine whether cells are indeed arrested in the following G1 phase in a p53-depenent manner, pre-synchronized IMR90 and IMR90 E6E7 cells were collected by mitotic shake-off after colcemid treatment and grown for 20 h followed by a 4 h BrdU incorporation interval (Fig. 6d). Both cell types accumulated TIF during prolonged mitotic arrest, confirming that p53 negative IMR90 cells were still competent of meta-TIF formation (Supplementary Fig. 5b). Both populations released at the 10 h time point efficiently incorporated BrdU after a 20 h recovery period, indicating that they entered the next round of the cell cycle (Fig. 6e, middle panel). When cells were released at the 16 h time point, IMR90 cells did not incorporate BrdU, while IMR90 E6E7 cells incorporated BrdU but displayed an increasing population of BrdU positive cells with polyploid DNA content (Fig. 6e, right panel). The diploid DNA content of the IMR90 cells released at the 10 and 16 h time points suggests that they progressed through cytokinesis (Supplementary Fig. 5c), which argues against the possibility that tetraploidy is required for the cell cycle arrest that follows prolonged mitotic arrest [29]. Our results support the hypothesis that in the presence of a functional p53 pathway, cells with extensive meta-TIF succumb to a growth arrest in the following G1 phase of the cell cycle. Contrary, when the p53 pathway is compromised, the cells continue progression through the cell cycle and become aneuploid.

To examine whether mitotic telomere deprotection causes telomere fusions in either the same mitosis or the following cell cycle, pre-synchronized IMR90 E6E7 cells were treated with colcemid, shaken-off at the 10 and 24 h time points and monitored for telomeric fusions after a 24 and 48 h recovery period. No increase of telomeric fusions during and after prolonged mitotic arrest was noted (Supplementary Fig. 5d). This indicates that telomere deprotection does not cause telomeric fusion during mitosis and the following cell cycle phase, which is consistent with the finding that partial TRF2 loss allows telomeres to be recognized as damage without resulting in chromosome fusions [8]. The lack of fusions in a scenario that displays overhang loss is inconsistent with the suggestion that NHEJ (Non

Homologous End Joining) dependent chromosome ligation is required for removal of the telomeric overhangs [30]. We suggest that the incomplete removal of TRF2 from telomeres during mitotic arrest, compounded with the absence of NHEJ activity during mitosis and the subsequent re-establishment of protection in the following G1 phase after release from mitotic arrest account for the differences in findings.

The Meta-TIF phenotype depends on Aurora B kinase activity

The phases of mitosis are monitored by the SAC, which prevents anaphase onset by targeting the APC, when the chromosomes fail to attach to spindle microtubules [31]. Aurora B kinase is critical in the correction of the microtubule mal-attachments and is involved in SAC signaling [31,32]. To test whether the SAC pathway is involved in mitotic telomere deprotection we targeted Aurora B by Hesperadin in the presence of Velcade. Velcade inhibits proteolysis of APC substrates, thereby canceling the requirement for SAC dependent mitotic arrest. Staining with the MPM-2 (Mitotic Phospho Marker 2) showed that Hesperadin strongly inhibited mitotic arrest induced by Taxol, verifying SAC inactivation (Fig. 7a, b). In Velcade-treated cells, Hesperadin prevented H3-Ser10P as consequence of Aurora B inhibition, and Aurora A Inhibitor I, used as a control, prevented Aurora A autophosphorylation, emphasizing their specificity (Supplementary Fig. 6c). In this setting, Hesperadin, but not Aurora A Inhibitor I, prevented the accumulation of meta-TIF (Fig. 7c, d), suggesting that mitotic telomere deprotection is dependent on Aurora B kinase activity. Aurora B inhibited cells were still competent for DNA damage signaling upon 1 Gy irradiation, excluding the possibility that Hesperadin inhibits ATM activity (Supplementary Fig. 6d, e). We were not able to test whether continuous Aurora B inhibition after a velcade wash-out had an effect on telomeric TRF2 or on the telomere protection status, since these experimental conditions led to anaphase and cytokinesis failure, comparable to a prolonged Aurora B knockdown [33].

To distinguish between a role of Aurora B or the SAC in meta-TIF formation we exposed velcade treated cells to reversine, which inhibits MPS1 (MonoPolar Spindle 1) and therefore the SAC [34], but does not alter Aurora A or B activity at the concentrations used (Supplementary Fig. 6c). Reversine dependent MPS1 suppression inhibited mitotic arrest induced by Taxol as expected (Fig. 7b), but failed to suppress telomeric damage foci formation in velcade treated cells (Fig. 7c, d), which indicates that Aurora B, but not the SAC pathway is involved in the meta-TIF induction. These results indicate that telomere deprotection after prolonged mitotic arrest is a programmed response ensuring DNA damage checkpoint activation and cell growth arrest.

Discussion

Here we describe a checkpoint pathway that is triggered following prolonged mitotic arrest. We propose a model, where prolonged mitotic duration results in destabilization of the telomere binding protein TRF2 causing telomere dysfunction and activation of a DNA damage response at chromosome ends. When activated in primary cells this checkpoint leads to cell cycle arrest and apoptosis in the following G1 phase of the cell cycle (Fig. 8). If activated in transformed cells this checkpoint could send transformed cells on a path to

aneuploidy. Previous observation reported that mitotic arrest is associated with the formation of chromosomal γ-H2AX foci, but the cause of this DNA damage response was obscure [35,36]. We propose a model where partial loss of TRF2 during mitotic arrest triggers an ATM-dependent damage response and degradation of the telomeric G-strand overhang.

Our model dictates a simple and effective mechanism to induce the DNA damage response pathway resulting in the exposure of telomeric ends to the DNA damage checkpoint machinery. It remains unclear specifically how TRF2, or potentially other shelterin components are removed from telomeres, however, we suspect an active process, involving mitosis-specific posttranslational modifications of TRF2. It is possible that factors, such as phosphatases, which inhibit putative modification of TRF2 antagonize Aurora B kinase-dependent telomere deprotection and are subjected to gradual degradation during prolonged mitotic arrest, controlling time dependence of TRF2 removal from telomeres. It is also possible that Aurora B activity at telomeres increases as a correlation of time spent in mitosis, and when a threshold is exceeded, TRF2 gets modified and removed.

Mitotic inhibitors are frequently used during treatment of a wide variety of cancers, and mitosis progression has long been viewed as an attractive target for the development of novel therapeutic candidates [37]. While it has not been understood what the mechanism for the induction of cell death upon mitotic inhibition is, it has been proposed that the p53 dependent checkpoint upon spindle disruption overlaps with the p53 dependent checkpoint following DNA damage [38]. Here we propose that telomere deprotection is the universal signal that initiates the DNA damage response upon failure to complete mitosis.

Our finding that cells with a competent p53 pathway arrest in G1 after release or escape from mitotic arrest, whereas cells lacking functional p53 and Rb pathways continue to cycle in the presence of DNA damage signaling offers an explanation why transformed cells are more sensitive to mitotic inhibitors than primary cells. However, the finding that telomere deprotection is the initiating signal for the damage response upon mitotic inhibition also raises caution for the use of such drugs, as cells that escape the mitotic block will inevitably suffer from telomere deprotection and are prone to become aneuploid. On the other hand, it could be beneficial to combine mitotic inhibitors with drugs that sensitize cells to active damage signaling. Furthermore, considering that a loss of the 3’-overhang is the initiating signal for the damage response it might be effective to combine mitotic inhibitors with telomerase inhibitors, as telomerase has the capability to regenerate a 3’-overhang at chromosome ends.

Methods

Cell Culture and Treatments

Human IMR90 primary lung fibroblasts (ATCC), A-T fibroblasts (GM09607 and GM01588; Coriell) and Seckel syndrome fibroblasts (GM09812; Coriell) were grown in Glutamax-DMEM (Gibco) supplemented with 0.1 mM Nonessential Amino Acids and 15% v/v Fetal Bovine Serum. HMECs (Lonza) cells were grown in SAGM™ Small Airway Epithelial Cell Growth Medium (CC-3118; Lonza). HeLa1.2.11 cells were grown in Glutamax-DMEM supplemented with 0.1 mM Nonessential Amino Acids and 10% v/v

Bovine Growth Serum. All cells were grown at 7.5% v/v CO_2 and 3% v/v O_2. IMR90, A-T cells (GM01588) and Seckel fibroblasts (GM09812) were infected with HPV16 E6 and E7 vectors as described [39]. For immunofluorescence cells were grown on Alcian blue (Sigma)-treated coverslips.

Synchronization was performed as described [40], except for using thymidine for the second block. Where indicated, 20 ng ml^{-1} or 100 ng ml^{-1} colcemid (Invitrogen), 100 nM Vinblastine (A. G. Scientific, Inc.), 500 nM Taxol (A. G. Scientific, Inc.), 1 μM Dimethylenastron (A. G. Scientific, Inc.), 1 μM Velcade-Bortezomib (Selleck), 250 nM Hesperadin (Selleck), 3 μM Aurora A Inhibitor I (Selleck) or 0.5 μM Reversine (Selleck) were supplied to the medium; or cells were irradiated with 1 Gy γ-irradiation 30 min prior to harvesting.

FACS analysis was performed as described [3]. For mitotic index analysis, cells were treated with Alexa-488 conjugated anti-histone H3-Ser10P antibody (9708, Cell Signaling Technology) and 7-AAD (BD Biosciences) according to manufacture's instructions. For cycling population analysis, cells were grown for 4 h in the presence of 10 μM BrdU (Sigma) before 70% v/v ethanol fixation and treated with Alexa-488 conjugated anti-BrdU antibody (BD Biosciences) and Propidium Iodide.

Transfections

We transiently transfected plasmid DNA using Lipofectamine 2000 (Invitrogen) and siRNA using Dharmafect (Dharmacon) according to manufacture's instructions. RAD21 siRNAs were transfected 48 h prior to harvest and sororin-shugoshin siRNAs 24 h prior to harvest. For transient ATM knockdown, 2 μg ml^{-1} puromycin (Sigma) was added to the medium at 24 h time point post transfection and cells were selected for 48 h. Colcemid was added at 48 or 70 h time point post transfection.

Viral Infections

Lentiviral vectors pseudotyped with VSV glycoprotein were generated by the Salk Institute Viral Vector Core using a protocol modified from [41]. IMR90 E6E7 cells were plated in growth media containing 4 μg ml^{-1} polybrene (Sigma) and lentivirus at an MOI of 10 and cultured for two days. The cells were then split into media containing 1 μg ml^{-1} puromycin and selected for five days before experimentation.

Plasmids and siRNA

Plasmids: pLPC and pLPC-TRF2 (ref. 26); pGIPZ-shRNAmir against ATM (Open Biosystems, sense sequence 5'-CCTATATCAGCAATTGTCA-3'); pGIPZ non-silencing shRNAmir control vector; pLKO.1 TRCN0000018358 shRNA against TRF2 (Open Biosystems, sense sequence 5'-ACAGAAGCAGTGGTCGAATC-3'); pLKO.1 scramble shRNA (sense sequence 5'-CCTAAGGTTAAGTCGCCCTCG-3') [42]. ON-TARGETplus SMARTpool siRNA against human RAD21, SGOL1 (Shugoshin) and CDCA5 (Sororin) were purchased from Thermo Scientific and used at manufacture's instruction.

Antibodies

Primary antibodies: anti-γ-H2AX (613402 clone 2F3, Biolegend); anti-H2AX (ab11175, Abcam); anti-RAD21 (J.M. Peters); anti-Sororin FL-252 (sc-67247, Santa Cruz Biotechnology); anti-Shugoshin (ab21633-100, Abcam); anti-γ-Tubulin (T6557, SIGMA); anti-Actin (A1978, SIGMA); anti-RAP1 (A300-306A, Bethyl Laboratories); anti-TRF1, 2 (Karlseder lab); anti-TIN2, anti-TPP1 (T. de Lange); anti-POT1 (P. Baumann); anti-p53 (sc126, Santa Cruz Biotechnology); anti-p53-ser15 (9284, Cell Signaling Technology); anti-p21 (05-345, Millipore); anti-histone H3 (ab1791, Abcam); anti-histone H3-Ser10P (3377, Cell Signaling Technology); anti-ATM (1549-1, Epitomics); anti-ATM-Ser1981P (200-301-400, Rockland); anti-phospho-SerThr-Pro, MPM-2 (05-368, Millipore); anti-phospho-Aurora A Thr288 (C39D8, Cell Signaling).

Secondary antibodies: HPR-linked anti-mouse or anti-rabbit (NXA931 or NA934V; GE Healthcare); Alexa-488-conjugated anti-mouse or anti-rabbit (Invitrogen); Alexa-594-conjugated anti-mouse or anti-rabbit (Invitrogen).

Western Blotting

Western blots were performed as described [43] with these minor alterations: cells were lysed at 1×10^4 cells per μl in NuPage LDS sample buffer (Invitrogen) containing 2% v/v β-Mercaptoethanol (Sigma) and 5% v/v Benzonase (Novagen) for 2 h at 37°, and 5% w/v Nonfat Milk in 1×PBS + 0.1% v/v Tween20 (Sigma) was used as a blocking agent. 70,000 cell equivalents were loaded per lane.

Immunofluorescence and Telomere FISH on Metaphase Spreads

We performed cytocentrifugation, IF and telomeric FISH and imaged metaphases as described [8].

Native and Denaturing Telomere Blots

Single and double stranded telomere analysis was performed as described [26].

Chromatin Immunoprecipitation

Chromatin immunoprecipitations were performed as described [44].

Metaphase Spreads for Quantification of Fusions

Percentage of telomere fusion per chromosome end was analyzed as described [8]. For 24 and 48 h time points post mitotic shake-off, cells were treated with 100 ng ml^{-1} colcemid in the last 1–2 h to accumulate mitotic cells without inducing the meta-TIF phenotype.

Supplementary Material

Refer to Web version on PubMed Central for supplementary material.

Acknowledgments

We thank J.M. Peters (Institute for Molecular Pathology), T. de Lange (The Rockefeller University) and P. Baumann (Stowers Institute for Medical Research) for antibodies, D. Gibbs (The Salk Institute) for production of

lentivirus and the Karlseder Laboratory for comments. MTH is supported by a Human Frontier Science Program Long Term Fellowship and a Japan Society for the Promotion of Science Postdoctoral Fellowships for Research Abroad. AJC is supported by a training grant from the NIH (5T32CA009370-29). This work was supported by the Cancer Center Core Grant P30 CA014195-38 and grants from the NIH to JK (AG025837, GM087476).

References

1. de Lange T. How telomeres solve the end-protection problem. Science. 2009; 326:948–952. [PubMed: 19965504]
2. van Steensel B, Smogorzewska A, de Lange T. TRF2 protects human telomeres from end-to-end fusions. Cell. 1998; 92:401–413. [PubMed: 9476899]
3. Karlseder J, Broccoli D, Dai Y, Hardy S, de Lange T. p53- and ATM-dependent apoptosis induced by telomeres lacking TRF2. Science. 1999; 283:1321–1325. [PubMed: 10037601]
4. Denchi EL, de Lange T. Protection of telomeres through independent control of ATM and ATR by TRF2 and POT1. Nature. 2007; 448:1068–1071. [PubMed: 17687332]
5. Guo X, et al. Dysfunctional telomeres activate an ATM-ATR-dependent DNA damage response to suppress tumorigenesis. EMBO J. 2007; 26:4709–4719. [PubMed: 17948054]
6. Takai H, Smogorzewska A, de Lange T. DNA damage foci at dysfunctional telomeres. Curr Biol. 2003; 13:1549–1556. [PubMed: 12956959]
7. d'Adda di Fagagna F, et al. A DNA damage checkpoint response in telomere-initiated senescence. Nature. 2003; 426:194–198. [PubMed: 14608368]
8. Cesare AJ, et al. Spontaneous occurrence of telomeric DNA damage response in the absence of chromosome fusions. Nat Struct Mol Biol. 2009; 16:1244–1251. [PubMed: 19935685]
9. Rieder CL, Maiato H. Stuck in division or passing through: what happens when cells cannot satisfy the spindle assembly checkpoint. Dev. Cell. 2004; 7:637–651. [PubMed: 15525526]
10. Brito DA, Rieder CL. Mitotic checkpoint slippage in humans occurs via cyclin B destruction in the presence of an active checkpoint. Curr. Biol. 2006; 16:1194–1200. [PubMed: 16782009]
11. Gascoigne KE, Taylor SS. Cancer cells display profound intra- and interline variation following prolonged exposure to antimitotic drugs. Cancer Cell. 2008; 14:111–122. [PubMed: 18656424]
12. Schvartzman JM, Sotillo R, Benezra R. Mitotic chromosomal instability and cancer: mouse modelling of the human disease. Nat. Rev. Cancer. 2010; 10:102–115. [PubMed: 20094045]
13. Ganem NJ, Storchova Z, Pellman D. Tetraploidy, aneuploidy and cancer. Curr Opin Genet Dev. 2007; 17:157–162. [PubMed: 17324569]
14. Ganem NJ, Pellman D. Limiting the proliferation of polyploid cells. Cell. 2007; 131:437–440. [PubMed: 17981108]
15. Michaelis C, Ciosk R, Nasmyth K. Cohesins: chromosomal proteins that prevent premature separation of sister chromatids. Cell. 1997; 91:35–45. [PubMed: 9335333]
16. Guacci V, Koshland D, Strunnikov A. A direct link between sister chromatid cohesion and chromosome condensation revealed through the analysis of MCD1 in S. cerevisiae. Cell. 1997; 91:47–57. [PubMed: 9335334]
17. Kitagawa R, Bakkenist CJ, McKinnon PJ, Kastan MB. Phosphorylation of SMC1 is a critical downstream event in the ATM-NBS1-BRCA1 pathway. Genes Dev. 2004; 18:1423–1438. [PubMed: 15175241]
18. Kim ST, Xu B, Kastan MB. Involvement of the cohesin protein, Smc1, in Atm-dependent and independent responses to DNA damage. Genes Dev. 2002; 16:560–570. [PubMed: 11877376]
19. Yazdi PT, et al. SMC1 is a downstream effector in the ATM/NBS1 branch of the human S-phase checkpoint. Genes Dev. 2002; 16:571–582. [PubMed: 11877377]
20. Watrin E, Peters JM. The cohesin complex is required for the DNA damage-induced G2/M checkpoint in mammalian cells. EMBO J. 2009; 28:2625–2635. [PubMed: 19629043]
21. Watrin E, et al. Human Scc4 is required for cohesin binding to chromatin, sister-chromatid cohesion, and mitotic progression. Curr Biol. 2006; 16:863–874. [PubMed: 16682347]
22. Schmitz J, Watrin E, Lenart P, Mechtler K, Peters JM. Sororin is required for stable binding of cohesin to chromatin and for sister chromatid cohesion in interphase. Curr Biol. 2007; 17:630–636. [PubMed: 17349791]

23. Downing KH. Structural basis for the interaction of tubulin with proteins and drugs that affect microtubule dynamics. Annu Rev Cell Dev Biol. 2000; 16:89–111. [PubMed: 11031231]
24. Shen L, et al. Cell death by bortezomib-induced mitotic catastrophe in natural killer lymphoma cells. Mol Cancer Ther. 2008; 7:3807–3815. [PubMed: 19074855]
25. Muller C, et al. Inhibitors of kinesin Eg5: antiproliferative activity of monastrol analogues against human glioblastoma cells. Cancer Chemother Pharmacol. 2007; 59:157–164. [PubMed: 16703323]
26. Karlseder J, Smogorzewska A, de Lange T. Senescence induced by altered telomere state, not telomere loss. Science. 2002; 295:2446–2449. [PubMed: 11923537]
27. Sfeir A, et al. Mammalian telomeres resemble fragile sites and require TRF1 for efficient replication. Cell. 2009; 138:90–103. [PubMed: 19596237]
28. Giunta S, Belotserkovskaya R, Jackson SP. DNA damage signaling in response to double-strand breaks during mitosis. J Cell Biol. 2010; 190:197–207. [PubMed: 20660628]
29. Andreassen PR, Lohez OD, Lacroix FB, Margolis RL. Tetraploid state induces p53-dependent arrest of nontransformed mammalian cells in G1. Mol. Biol. Cell. 2001; 12:1315–1328. [PubMed: 11359924]
30. Celli GB, de Lange T. DNA processing is not required for ATM-mediated telomere damage response after TRF2 deletion. Nat Cell Biol. 2005; 7:712–718. [PubMed: 15968270]
31. Musacchio A, Salmon ED. The spindle-assembly checkpoint in space and time. Nat Rev Mol Cell Biol. 2007; 8:379–393. [PubMed: 17426725]
32. Santaguida S, Vernieri C, Villa F, Ciliberto A, Musacchio A. Evidence that Aurora B is implicated in spindle checkpoint signalling independently of error correction. EMBO J. 2011; 30:1508–1519. [PubMed: 21407176]
33. Kim HJ, Cho JH, Quan H, Kim JR. Down-regulation of Aurora B kinase induces cellular senescence in human fibroblasts and endothelial cells through a p53-dependent pathway. FEBS Lett. 2011; 585:3569–3576. [PubMed: 22024481]
34. Santaguida S, Tighe A, D'Alise AM, Taylor SS, Musacchio A. Dissecting the role of MPS1 in chromosome biorientation and the spindle checkpoint through the small molecule inhibitor reversine. J Cell Biol. 2010; 190:73–87. [PubMed: 20624901]
35. Dalton WB, Nandan MO, Moore RT, Yang VW. Human cancer cells commonly acquire DNA damage during mitotic arrest. Cancer Res. 2007; 67:11487–11492. [PubMed: 18089775]
36. Quignon F, et al. Sustained mitotic block elicits DNA breaks: one-step alteration of ploidy and chromosome integrity in mammalian cells. Oncogene. 2007; 26:165–172. [PubMed: 16832348]
37. Janssen A, Medema RH. Mitosis as an anti-cancer target. Oncogene. 2011
38. Lanni JS, Jacks T. Characterization of the p53-dependent postmitotic checkpoint following spindle disruption. Mol Cell Biol. 1998; 18:1055–1064. [PubMed: 9448003]
39. Halbert CL, Demers GW, Galloway DA. The E7 gene of human papillomavirus type 16 is sufficient for immortalization of human epithelial cells. J Virol. 1991; 65:473–478. [PubMed: 1845902]
40. Crabbe L, Verdun RE, Haggblom CI, Karlseder J. Defective telomere lagging strand synthesis in cells lacking WRN helicase activity. Science. 2004; 306:1951–1953. [PubMed: 15591207]
41. Tiscornia G, Singer O, Verma IM. Production and purification of lentiviral vectors. Nat Protoc. 2006; 1:241–245. [PubMed: 17406239]
42. Sarbassov DD, Guertin DA, Ali SM, Sabatini DM. Phosphorylation and regulation of Akt/PKB by the rictor-mTOR complex. Science. 2005; 307:1098–1101. [PubMed: 15718470]
43. O'Sullivan RJ, Kubicek S, Schreiber SL, Karlseder J. Reduced histone biosynthesis and chromatin changes arising from a damage signal at telomeres. Nat Struct Mol Biol. 2010; 17:1218–1225. [PubMed: 20890289]
44. Verdun RE, Karlseder J. The DNA damage machinery and homologous recombination pathway act consecutively to protect human telomeres. Cell. 2006; 127:709–720. [PubMed: 17110331]

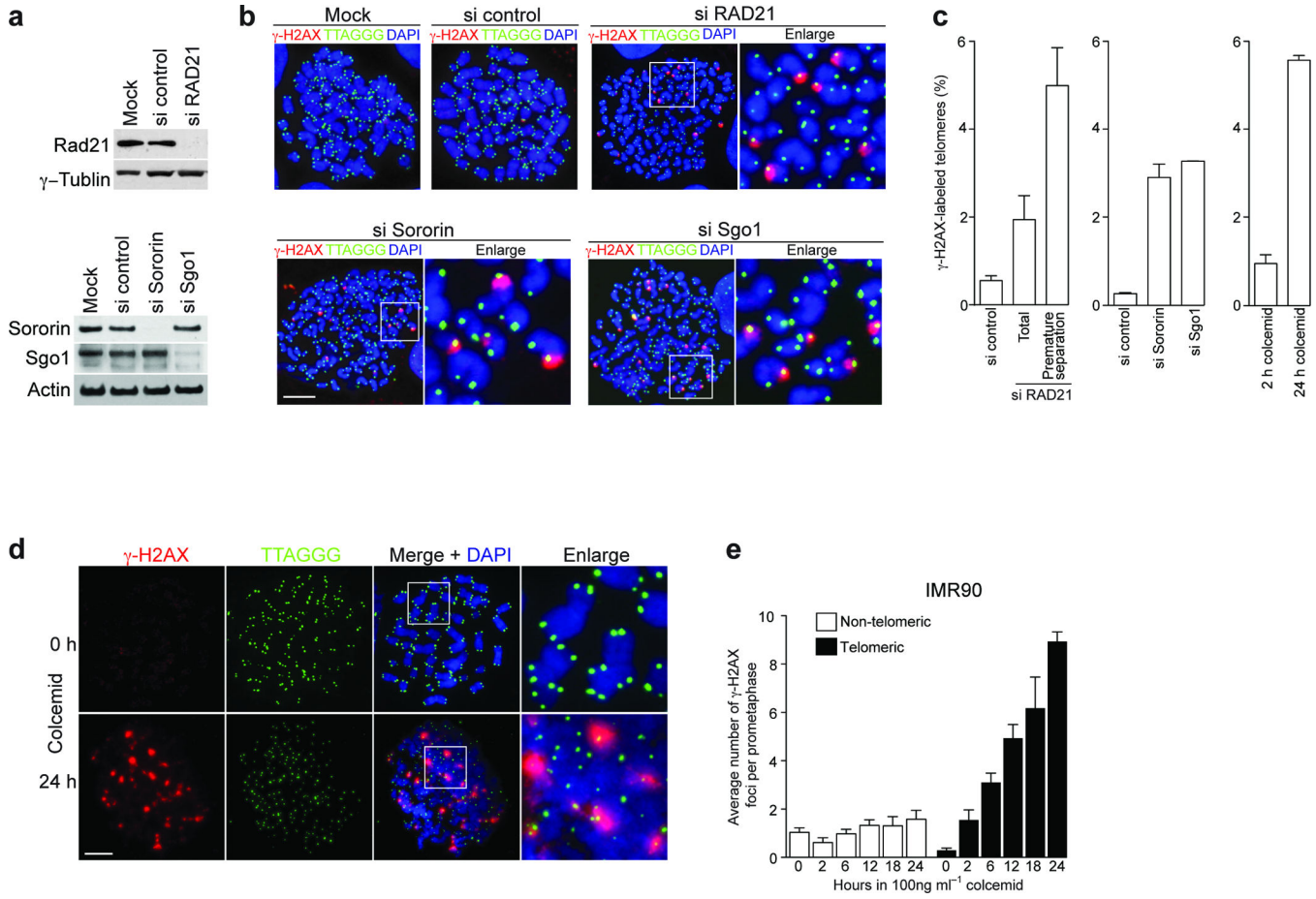

Figure 1.

Prolonged mitotic arrest causes telomere deprotection. **(a)** Western analysis of HeLa1.2.11 cells transfected with control siRNAs or siRNAs targeting RAD21, Sororin or Shugoshin (Sgo1). RAD21 has been targeted for 48 h, Sororin and Shugoshin for 24 h. γ-Tubulin and Actin serve as loading controls. **(b)** Immunofluorescence analysis of HeLa1.2.11 metaphase cells transfected with control siRNAs or siRNAs targeting RAD21, Sororin or Shugoshin. **(c)** Quantification of γ-H2AX positive telomeres in HeLa1.2.11 cells transfected as in panel **a**. The mean and standard deviation of three experiments quantifying 25 metaphases is shown. For RAD21 the percentages of γ-H2AX positive telomeres in all metaphases and metaphases that carry prematurely separated chromatids have been indicated, for Sororin and Shugoshin only the percentage in all metaphases is shown. γ-H2AX positive metaphase telomeres of HeLa1.2.11 cells treated with 100 ng ml^{-1} colcemid for 2 or 24 h are shown on the right. See also Supplementary Fig. 1a. **(d)** Immunofluorescence staining of metaphase chromosomes of IMR90 primary fibroblasts treated with colcemid for 0 hours or 24 hours. See also Supplementary Fig. 1b. **(e)** Quantification of γ-H2AX foci in IMR90 fibroblast prometaphases following the indicated treatment, displayed as in panel **c**. The mean and standard deviation of three experiments quantifying at least 25 prometaphases is shown. Scale bar, 10 μm.

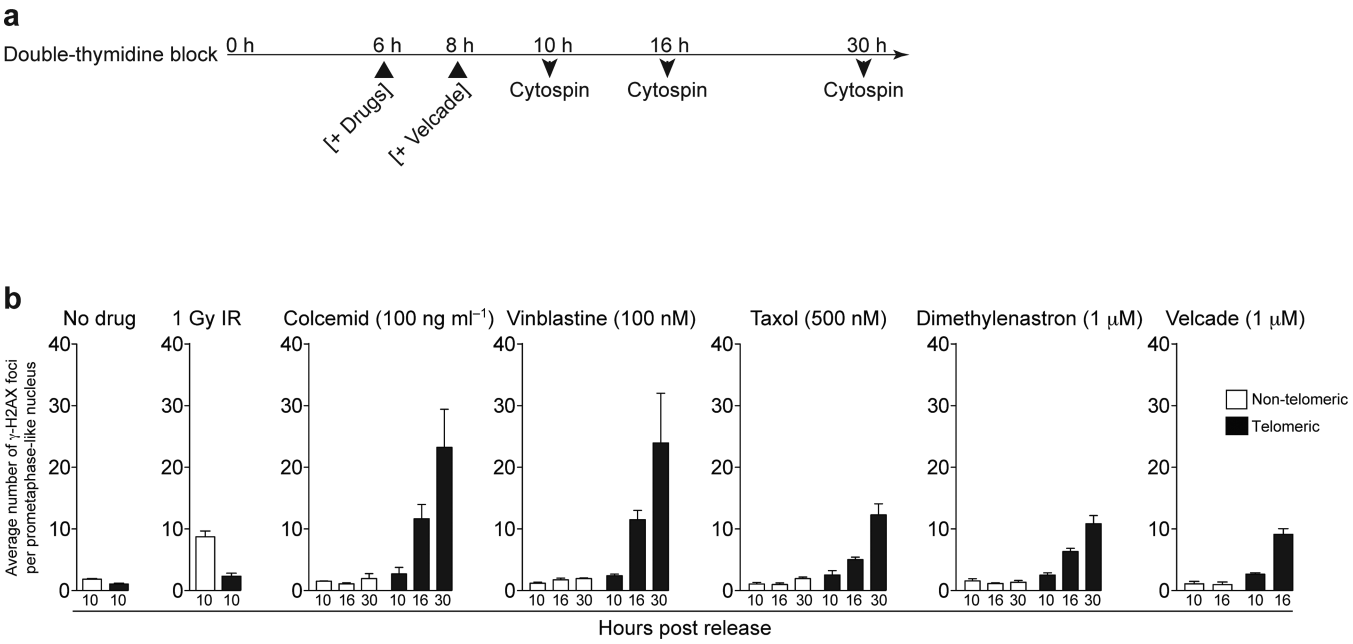

Figure 2.

Mitotic inhibitors cause telomere deprotection. **(a)** Schematic of the timing of experiments in panel **b**. **(b)** Quantification of γ-H2AX positive foci in prometaphase IMR90 cells following the indicated treatment. The mean and standard deviation of three experiments quantifying at least 25 prometaphases is shown.

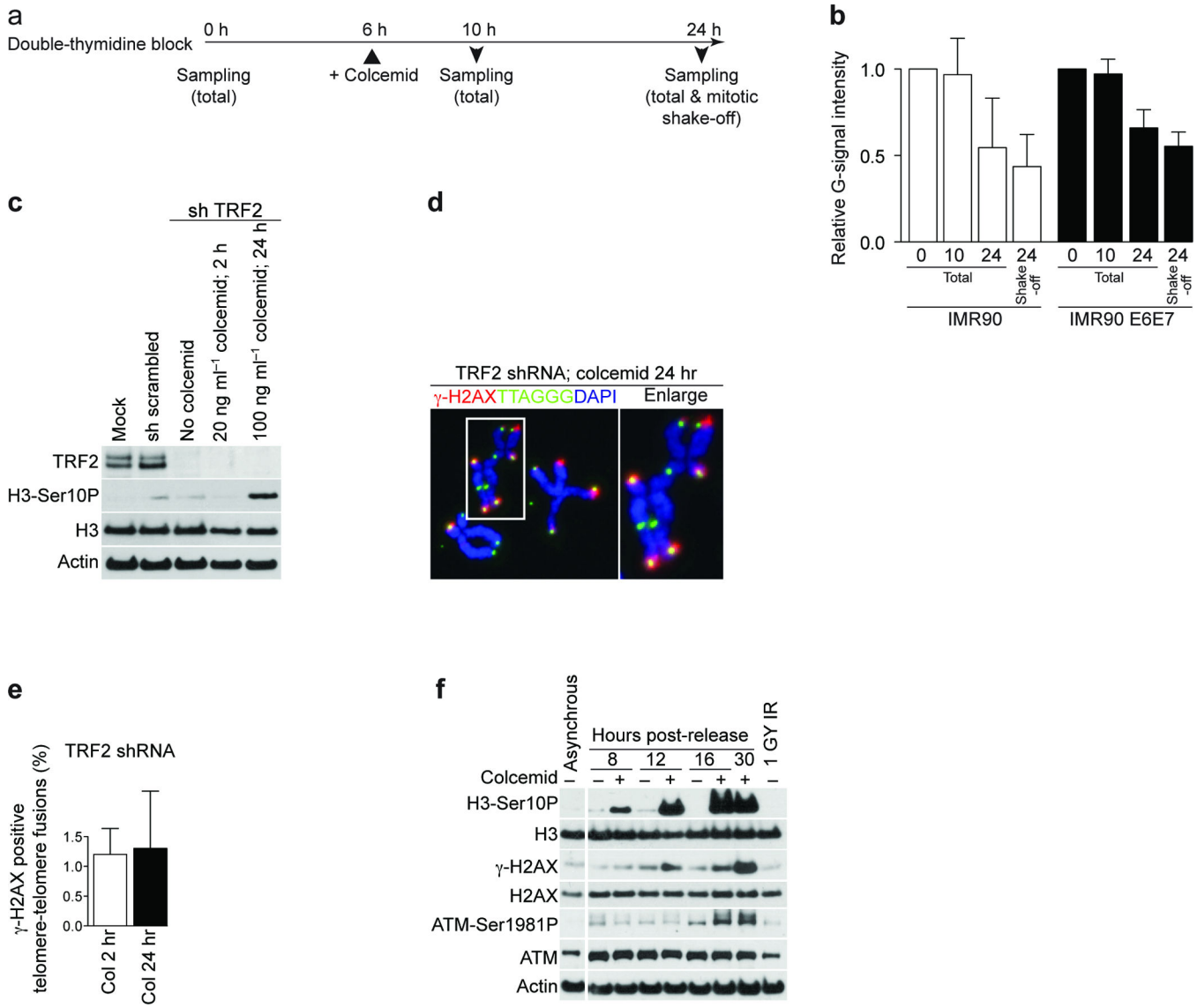

Figure 3.

Prolonged mitotic arrest causes the loss of 3'-overhangs and ATM activation. (**a**) Schematic of the timing of experiments in panel **b**. (**b**) Quantification of the ratio between native and denatured signals from telomeric southern analysis of IMR90 cells (white bars) or IMR90 E6E7 cells (black bars). The mean and standard deviation of three experiments is shown. (**c**) Western analysis of mock treated IMR90 E6E7 fibroblasts and cells expressing a scrambled shRNA or a shRNA targeting TRF2 with or without the indicated colcemid treatment. (**d**) Immunofluorescence image of metaphase chromosomes from IMR90 E6E7 cells with suppressed TRF2, exposed to 100 ng ml-1 colcemid for 24 hrs. (**e**) Quantification of γ-H2AX positive telomere fusions in IMR90 cells with suppressed TRF2, exposed to 20 ng ml-1 colcemid for 2 h or 100 ng ml-1 colcemid for 24 h. The mean and standard deviation of three experiments quantifying at least 135 fusions per experiment is shown. (**f**) Western analysis of asynchronous IMR90 fibroblasts and IMR90 cells released from G1-S arrest as shown. Where indicated, colcemid has been added 6 h after release.

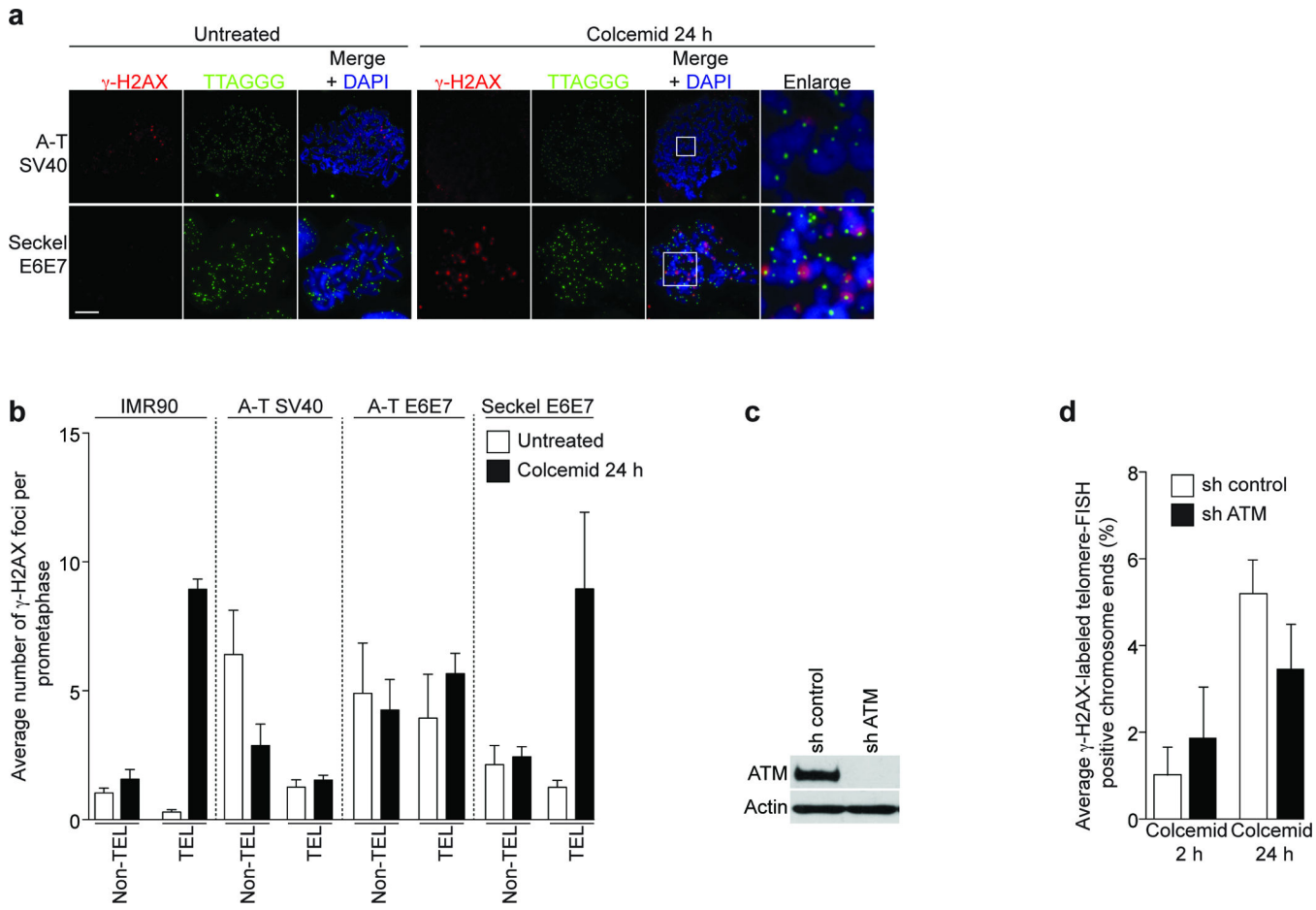

Figure 4.

Mitotic TIF formation is ATM dependent. (**a**) Immunofluorescence staining of A-T SV40 and Seckel E6E7 fibroblasts treated with colcemid for 24 h. Magnifications of indicated regions are on the right. (**b**) Quantification of γ-H2AX foci in IMR90, A-T SV40, A-T E6E7 and Seckel E6E7 metaphases. Displayed as in Fig. 1e. The mean and standard deviation of three independent experiments of 25 or more metaphases is shown. (**c**) Western analysis of ATM targeting in HeLa1.2.11 cells. (**d**) Quantification of meta-TIF in ATM targeted HeLa1.2.11 cells. Displayed as in Fig 1c. Scale bar, 10 μm.

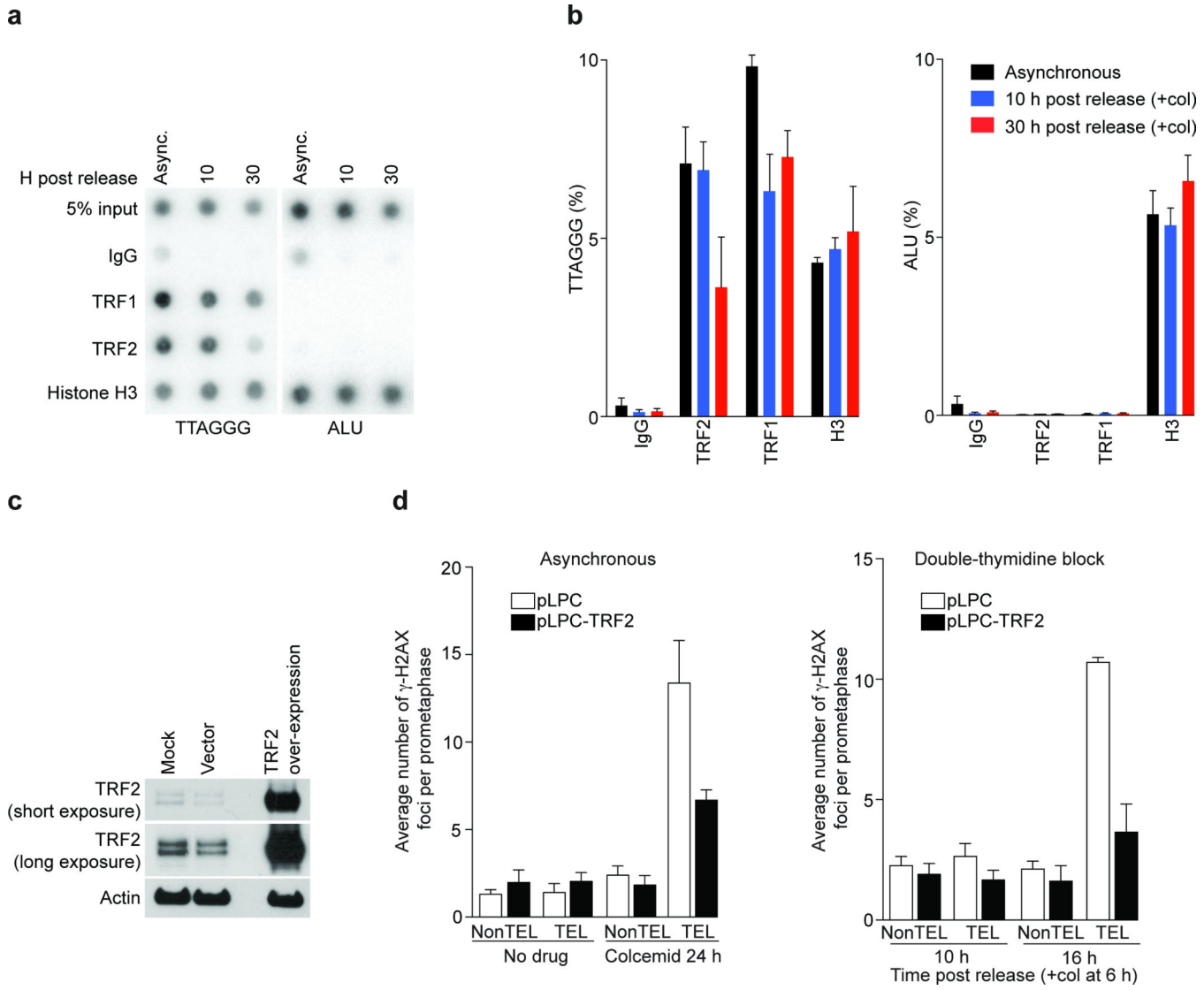

Figure 5.

Mitotic TIF are dependent on TRF2 removal. (**a**) Chromatin immunoprecipitation experiments from asynchronous IMR90 cells and synchronized IMR90 cells 10 and 30 h post release. Colcemid was added 6 h post release. Antibodies are indicated on the left and 5% of the input is shown. (**b**) Mean and standard error of three experiments as shown in panel **a**. (**c**) Western analysis of TRF2 overexpression in IMR90 cells. (**d**) Quantification of γ-H2AX foci in prometaphases from control and TRF2 overexpressing IMR90 cells in asynchronous (24 h of colcemid) and synchronized (10 and 16 h post release) populations. Displayed as in Fig. 1e.

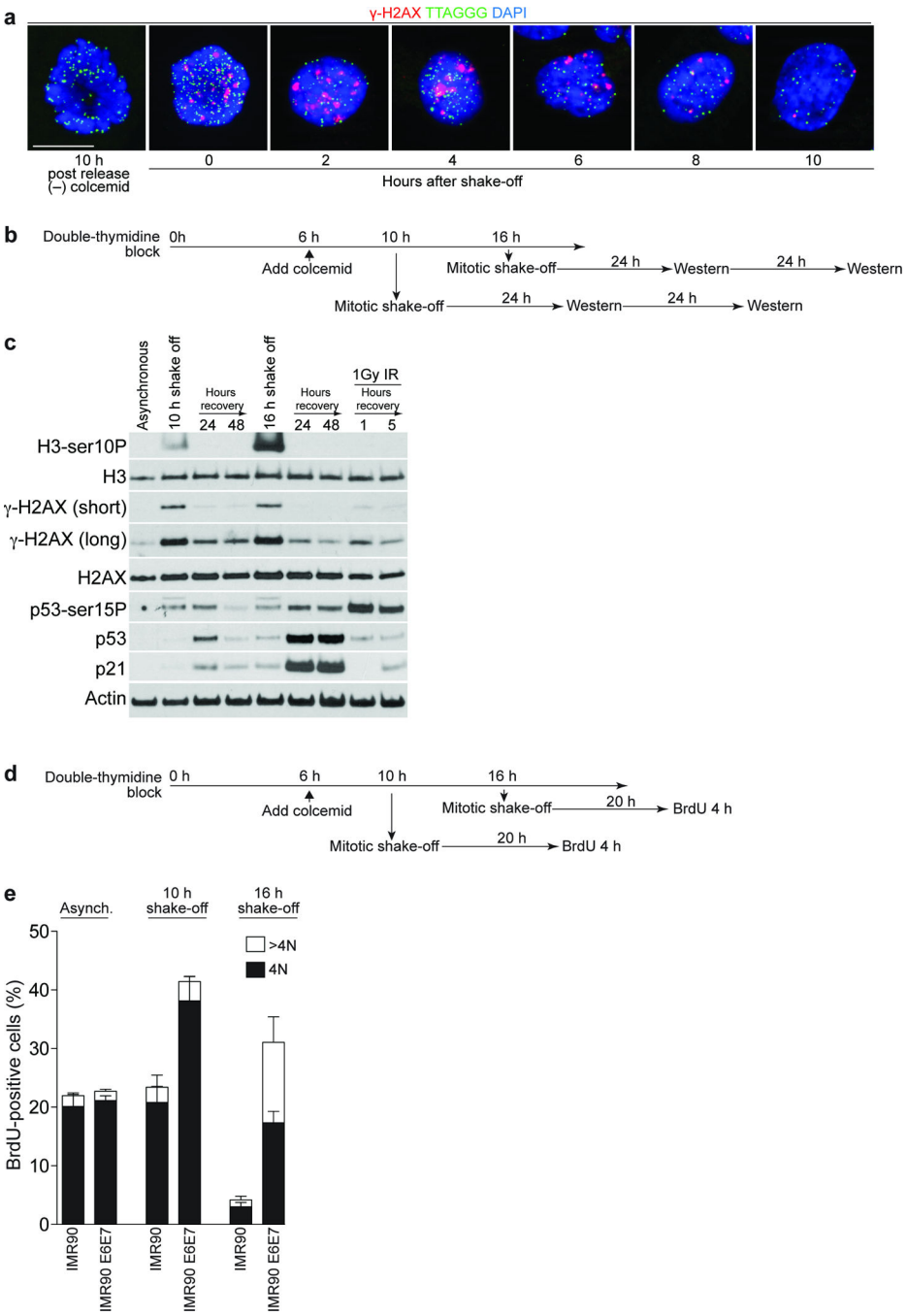

Figure 6.

Checkpoint activation by mitotic telomere deprotection. (**a**) Immunofluorescence of synchronized IMR90 cells treated with 100 ng ml-1 colcemid 6 h post release, cultured for 18 h before collection by shake-off. The cells were replated and fixated at the indicated times. A mitotic cell 10 h post-release without colcemid serves as the negative control. (**b**) Schematic of the timing of the experiment in panel **c**. (**c**) Western analysis of asynchronous IMR90 cells or IMR90 cells synchronized and collected as in panel **b**. Antibodies used are indicated on the left. (**d**) Schematic of the timing of the experiment in panel **e**. (**e**)

Quantification of BrdU-positive cells in asynchronous IMR90 and synchronized IMR90 and IMR90 E6E7 populations treated as in panel **d**. BrdU incorporation and DNA content was determined by FACS analysis. The mean and standard deviation of three independent experiments (20,000 cells analyzed per time point) is shown. Scale bar, 10 μm.

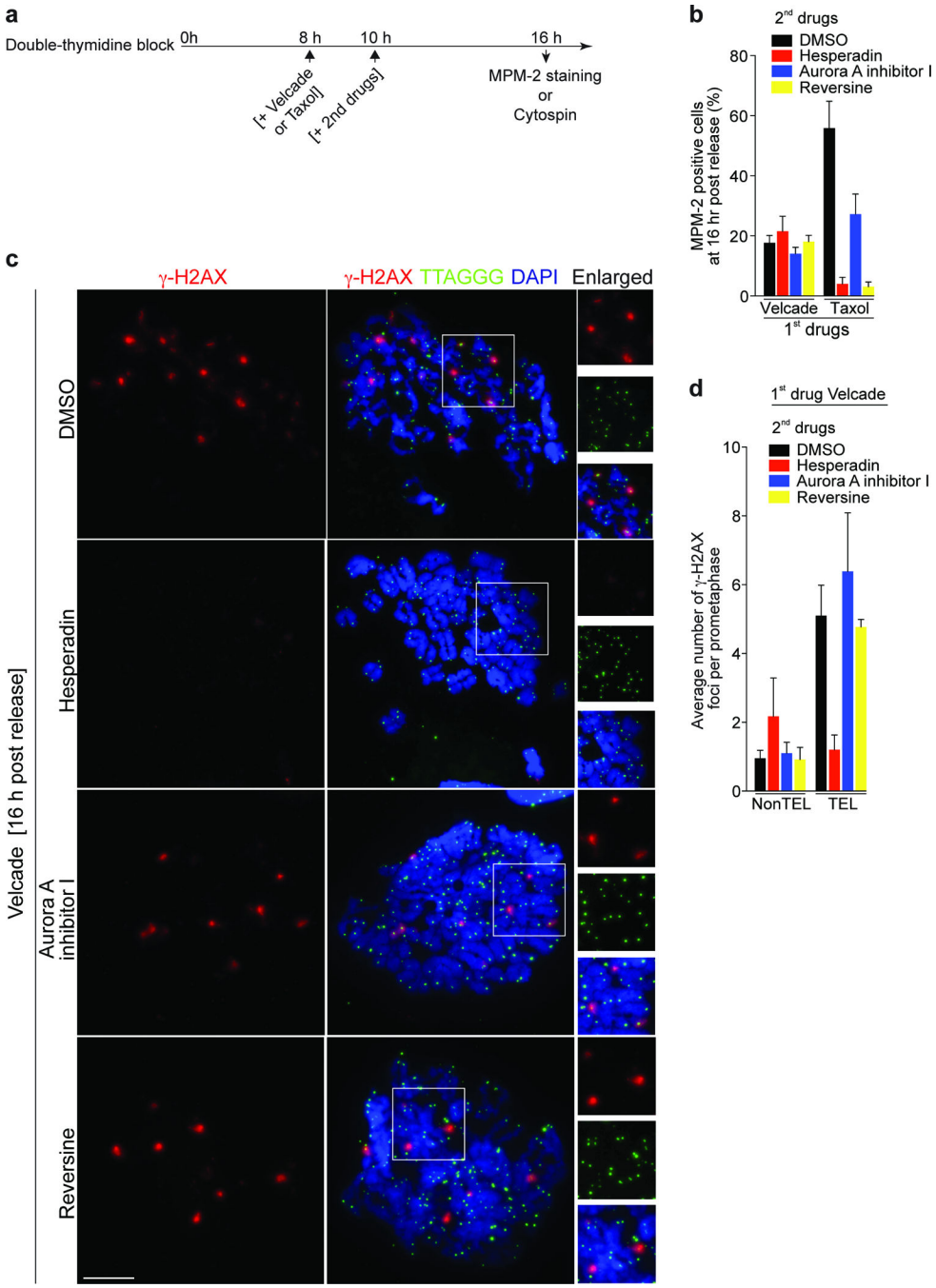

Figure 7.

Mitotic TIF formation is dependent on Aurora B kinase but not on the SAC. (**a**) Schematic of the timing of experiments in panels **b-d**. (**b**) Quantification of MPM-2 positive IMR90 cells that were first treated with 1μM Velcade or 500 nM Taxol, then control-treated with DMSO, with Hesperadin (250nM), Aurora A inhibitor I (3 μM) or Reversine (0.5 μM). (**c**) Meta-TIF analysis of IMR90 cells treated as indicated in panel **d**. Quantification of γ-H2AX foci from panel **c**. Displayed as in Fig. 1e. Scale bar, 10 μm.

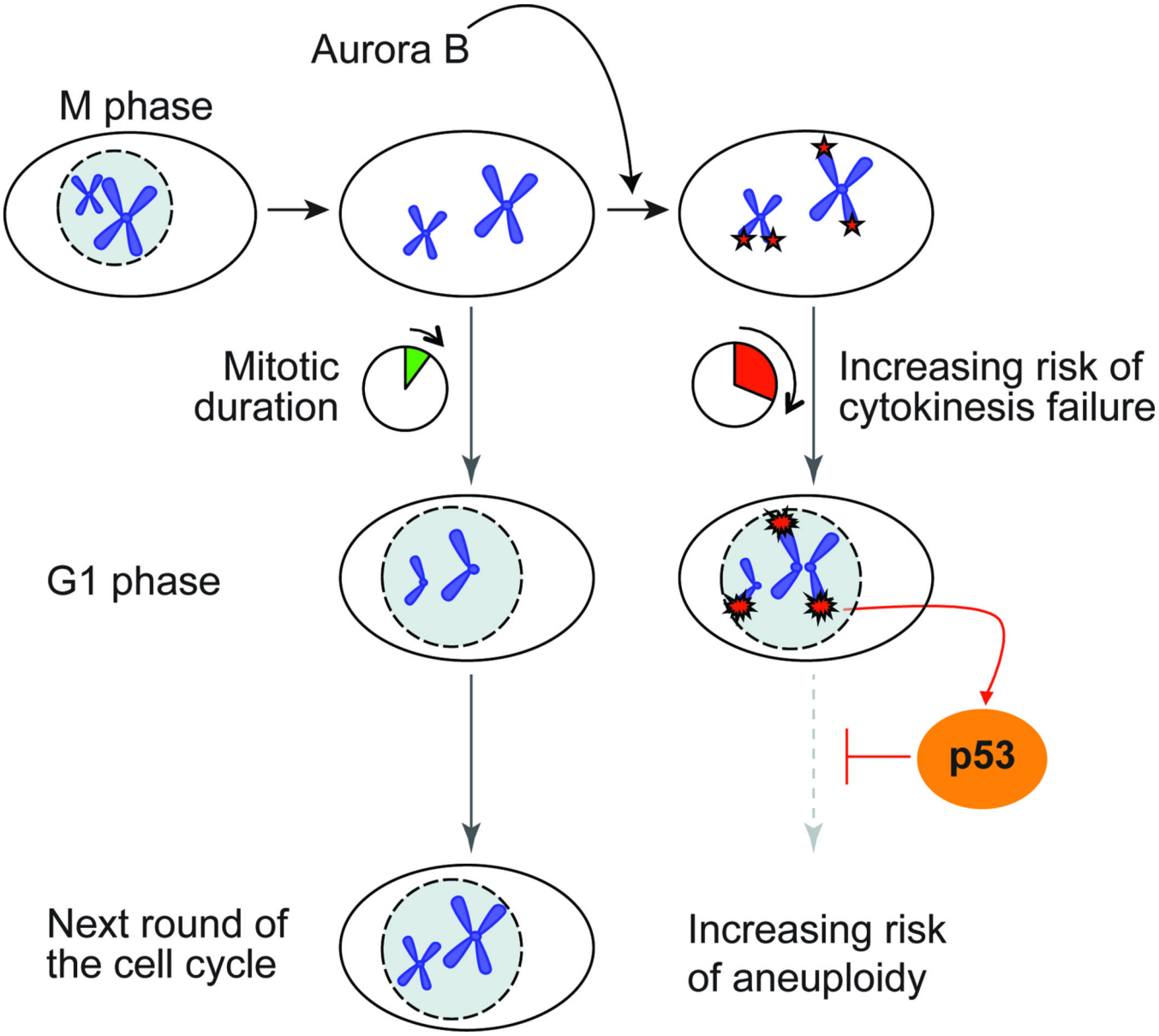

Figure 8.
Model for a telomere based mitotic duration checkpoint.